JOURNAL OF PROPULSION AND POWER
Vol. 9, No. 4, July–Aug. 1993

Temperature Control of a Liquid Helium Propulsion System

Peter Wiktor*
Stanford University, Stanford, California 94305

Two spacecraft, gravity probe B (GP-B) and the satellite test of the equivalence principle (STEP), incorporating onboard liquid helium cryogenic systems are scheduled to fly around the turn of the century. Effective propulsion systems can be implemented for these spacecraft by directing the helium gas which boils off from the cryogenic systems in specific directions through a set of thrusters. Due to extensive development and testing work, the ultra low flow rate helium thrusters for such a propulsion system are now considered proven technology. This article is concerned with implementing these thrusters into an effective overall propulsion system. A thermodynamic model relating the temperature, pressure, and flow rate of the propulsion system is derived. Based on this model a controller is developed which regulates the liquid helium supply temperature and pressure by varying the net helium mass flow rate through the thrusters. We show how the net mass flow rate can be controlled independently from the desired output thrust. The manifold pressure upstream of the thrusters is shown to remain remarkably stable even with fairly large flow rate variations. Using the GP-B spacecraft as an example we conclude that it is feasible to build a liquid helium based propulsion system with a very stable supply temperature and pressure.

Nomenclature

A = thruster configuration matrix
C_i = specific heat of $i = g, l, t$, J/mg·K
CM = thermal mass of system, J/K
c = plenum capacitance, mg/Pa
$\dot{E}_i$ = power of $i = s, o, i$, J/s
e = base of natural logarithms
$\boldsymbol{F}$ = 6 × 1 generalized force vector, mN
$\boldsymbol{F}_F$ = 3 × 1 force component, mN
$\boldsymbol{F}_M$ = 3 × 1 moment component, mN·m
h_{gl} = latent heat of vaporization, $h_g - h_l$, J/mg
h_i = enthalpy of $i = g, l$, J/mg
I_{sp} = specific impulse of thrusters, s
k_i = controller gain of $i = p, pp, ii$
k_{tp} = pressure vs temperature scale factor, Pa/K
m = number of degrees of freedom
n = number of thrusters
P_i = pressure at point $i = 0, \ldots, 5$, fep, Pa
P_{ij} = pressure drop between points $i, j = 0, \ldots, 5$, Pa
$\dot{Q}_i$ = heat flow to point $i = 0, h$, W
R = helium gas constant, J/kg·K
R_{ij} = flow resistance between points $i, j = 0, \ldots, 5$, Pa/(mg/s)
R_s = thermal resistance, K/W
$\mathcal{R}^m$ = m × 1 vector of reals
s = laplace operator
T_i = temperature of $i = o, c, m, s$
$\boldsymbol{T}_i$ = thrust command vector of $i = n, r$, mN
V = plenum volume, m³
v_e = exhaust gas velocity, $(9.8 \times 10^{-3})\, I_{sp}$, km/s
w = mass flow rate, mg/s
w_c = commanded mass flow rate, mg/s
Δ = variation or difference
η = helium gas viscosity, mg/m·s
ρ = helium gas density, mg/m³
τ = thermal time constant, s
ω = frequency, rad/s
ω_n = controller natural frequency, rad/s
$\mathbf{0}$ = vector of zeros

Subscripts
c = command
fep = fountain effect pump
g = gas
h = heater
i = input
ii = integral gain
l = liquid
m = measured
n = null space
o = output
p = passive system, peak or p norm
pp = proportional gain
r = particular solution
s = external shell of dewar
s = stored
t = tank
0 = liquid helium
1 = porous plug exit or 1 norm
2 = manifold
3 = thruster inlet
4 = nozzle inlet
5 = exit

Superscript
n = nominal

I. Introduction

THERE are at least two reasons to fly a liquid helium cryogenic system on a spacecraft. One is to increase the sensitivity of the detectors of orbiting telescopes like the infrared astronomical satellite (IRAS), the cosmic background explorer (COBE) and the space infrared telescope facility (SIRTF). The other reason is for thermal stability and for cooling of the superconducting quantum interference devices (SQUIDS) of orbiting gravitational experiments like gravity probe-B (GP-B)[1] and the satellite test of the equivalence principle (STEP).[2] As the liquid helium slowly boils off from the cryogenic systems of these spacecraft, the resulting helium gas must be vented overboard. The resulting thrust can easily be the largest disturbance to the attitude and translation con-

Received June 21, 1991; presented as Paper 91-3553 at the AIAA/SAE/ASME 27th Joint Propulsion Conference, Sacramento, CA, June 24–27, 1991; revision received April 17, 1992; accepted for publication Feb. 15, 1993.

*Research Assistant, Hansen Labs, GP-B.

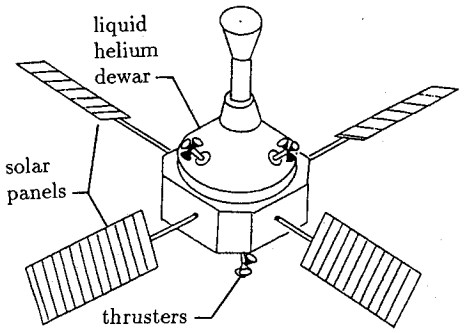

Fig. 1 Gravity probe B spacecraft with a liquid helium propulsion system.

trol systems of these spacecraft. During the preliminary design phase of the GP-B spacecraft, it was realized that instead of wasting the boil-off gas, it would be better to direct it through a set of thrusters.[3,4] The propellant for a spacecraft with a liquid helium cryogenic system (Fig. 1) is therefore essentially free.

The biggest hurdle in designing the liquid helium propulsion system is the design of the thrusters. In many ways the thrusters are a radical departure from conventional thruster designs. Their peak outputs are on the order of only 1–10 mN, Reynolds numbers are less than 100, and Knudsen numbers are greater than 0.1 in the thruster valve which means that the thrusters operate in a regime between slip and free molecular flow. Also, the output of the thrusters is proportional to a commanded value instead of the typical on-off output of conventional thrusters. Several prototypes of the proportional helium thrusters have been built and tested.[5–7] These tests have shown that it is indeed possible to operate a proportional thruster in a very low flow rate and pressure regime. Most significantly, the specific impulse has been measured to be at least 130 s at 300 K out of a theoretical maximum of 164 s.

This article is concerned with effectively incorporating the proportional thrusters into an overall propulsion system. First we deal with the control of the individual thrusters. The thrusters not only have to perform the conventional role of providing forces and moments for translation and attitude control, but in the case of a liquid helium propulsion system, they must also be able to vent the boil-off helium gas at a constant rate. We show how to send commands to the thrusters to obtain the desired forces and moments while at the same time obtaining a desired net flow rate. For a detailed discussion on optimizing the control of the thrusters to yield the greatest output thrust for a given mass flow rate see Refs. 8 and 9.

The two NASA spacecraft with onboard liquid helium cryogenic systems which have flown so far, IRAS and COBE, both vented their helium gas through a fixed output impedance. By commanding a constant flow rate the output impedance of a liquid helium propulsion system is also commanded to be fixed. However, due to thruster errors, the output impedance, and therefore, the true flow rate will constantly be changing. A linear thermodynamic model is derived to study how flow rate variations affect the temperature and pressure of the liquid helium. An active regulator which modulates the flow rate to control the liquid helium temperature and pressure is also derived. This controller can be used to boost the output of the thrusters for short periods of time based on the stored energy in the liquid helium. In Sec. VIII, the stability of the plenum pressure just upstream of the thrusters is studied.

II. Force Control

Thrusters are used on a spacecraft for attitude and translation control. The GP-B spacecraft, for example, will have up to 18 thrusters providing moments, $\boldsymbol{F}_M$, for attitude control around three axes and forces, $\boldsymbol{F}_F$, for translation control along three axes. The net force and moment exerted on the spacecraft by the combined outputs of the individual thrusters can be expressed as

$$\boldsymbol{F} = A\boldsymbol{T} \tag{1}$$

where $\boldsymbol{F}$ is a 6×1 generalized force vector composed of the 3 components of the force $\boldsymbol{F}_F$, and moment $\boldsymbol{F}_M$ vectors, respectively. If n is the number of thrusters then $\boldsymbol{T}$ is a $n \times 1$ vector of the magnitudes of the force exerted by the individual thrusters, and A is the $6 \times n$ configuration matrix which defines the positions and orientations of each thruster.

Since a thruster's output is one-sided, meaning that it can only output force in one direction, the thrusters must also satisfy the nonlinear constraint

$$\boldsymbol{T} \geq \boldsymbol{0} \tag{2}$$

where the inequality holds for each element of $\boldsymbol{T}$.

Given a desired generalized force $\boldsymbol{F}$ and a configuration matrix A, the thruster control problem consists of solving the set of simultaneous linear equations, $\boldsymbol{F} = A\boldsymbol{T}$, for the thrust vector $\boldsymbol{T}$, subject to the constraint [Eq. (2)]. Various solutions to this problem are outlined in Ref. 8; but how are we guaranteed that a solution exists? The following theorem defines the necessary and sufficient conditions which a thruster system must satisfy in order to be able to generate forces in any direction.

A. Theorem

A nonnegative solution

$$\boldsymbol{T} \geq \boldsymbol{0} \tag{3}$$

to

$$\boldsymbol{F} = A\boldsymbol{T} \tag{4}$$

exists for all $\boldsymbol{F} \in \mathcal{R}^m$ if and only if A has rank m and there exists a positive vector

$$\boldsymbol{T}_n > \boldsymbol{0} \tag{5}$$

in the null space of A

$$A\boldsymbol{T}_n = \boldsymbol{0} \tag{6}$$

B. Proof: Sufficient Condition

If A is full rank then there exists a solution, $\boldsymbol{T}_s$, to Eq. (4) for any $\boldsymbol{F} \in \mathcal{R}^m$

$$\boldsymbol{F} = A\boldsymbol{T}_s \tag{7}$$

In general, this solution has the form

$$\boldsymbol{T}_s = \boldsymbol{T}_r + \boldsymbol{T}_n \tag{8}$$

where $\boldsymbol{T}_r$ is the unique "particular" solution in the row space of A and $\boldsymbol{T}_n$ is in the null space, $A\boldsymbol{T}_n = \boldsymbol{0}$.

Since $\boldsymbol{T}_n$ doesn't affect the output, it can be made as big as needed to satisfy Eq. (3). As long as the smallest element of $\boldsymbol{T}_n$ is bigger than the largest absolute value of $\boldsymbol{T}_r$, then $\boldsymbol{T}_s = \boldsymbol{T}_r + \boldsymbol{T}_n \geq \boldsymbol{0}$.

C. Necessary Condition

We prove the necessary condition by contradiction.

1) If A is not full rank, rank$(A) < m$, then there exists some $\boldsymbol{F}$ such that Eq. (4) cannot be satisfied, $\boldsymbol{F} \neq A\boldsymbol{T}$.

2) There is at least one output vector, $\boldsymbol{F}$, corresponding to each vector, $\boldsymbol{T}_r$, of the particular solution [Eq. (8)]. In other words, any desired vector $\boldsymbol{T}_r$ can be obtained by selecting an appropriate output vector, $\boldsymbol{F}$.

If condition Eq. (5) does not hold then there exists some component of T_n which is less than or equal to zero, $(T_n)_i \leq 0$. A particular solution, T_r, with the corresponding ith element less than zero, $(T_r)_i < 0$, can be obtained by selecting an appropriate output vector, F. The ith element of the sum, $T_s = T_r + T_s$ is negative therefore, violating Eq. (3).

3) If A is full rank but does not have a nonpositive null space component, contradicting Eq. (5) then A is nonsingular and the unique solution to $F = AT$ is given by

$$T = A^{-1}F \tag{9}$$

If a given vector, F, results in a solution, T with a positive component then from Eq. (9) that component will be negative for $-F$, thus violating Eq. (3).

An interesting corollary of the Theorem in Sec. II.A. is that if a thruster can generate forces, F, in any direction then it must have at least $m + 1$ thrusters where m is the size of the vector F. This follows from the fact that the rank m matrix, A, must have at least $m + 1$ columns in order to have a nontrivial null space. This fact has also been proven independently by Chen[6] and Salisbury.[10] Having $m + 1$ thrusters by itself does not guarantee that the thruster system can generate forces in any direction. The necessary and sufficient conditions are given by the Theorem in Sec. II.A.

In general, a propulsion system can have more thrusters than degrees of freedom (DOF) $n > m$. This means that there can be an infinite number of solutions to the underdetermined set of linear equations [Eq. (1)]. By requiring the thrusters to satisfy some additional constraints, a unique solution can be specified. In Ref. 8, for example, we show how to control the thrusters so they can generate a desired output force while minimizing either the required mass flow rate, power or supply pressure.

III. Flow Control

The thrusters use the boil-off gas from the cryogenic liquid helium for their propellant. To maintain constant cooling this gas must be vented continuously. The thrusters must therefore perform two independent tasks: generate the desired forces and moments on the spacecraft and maintain the helium flow rate required for cooling. A simple thruster controller which accomplishes these tasks is defined in the following theorem. The key feature of this controller is that it first calculates the thrust command vector to generate the desired force and moment. It then calculates the additional flow rate needed to meet the cooling requirement and then dumps this flow into the null space of A. This does not disturb the spacecraft since thrust commands in the null space do not generate any forces and moments. The following theorem uses the 1-norm, $\|T\|_1$, which is defined as the sum of the absolute values of the elements of the vector T.

A. Theorem

Given A; a desired force F; a commanded net flow rate w_c; a scale factor between flow rate and force v_e; a thrust control vector T_p, which satisfies

$$F = AT_p \tag{10}$$

$$T_p \geq 0 \tag{11}$$

$$\|T_p\|_1 \leq w_c v_e \tag{12}$$

a vector, T_n, which lies in the null space of A

$$AT_n = 0 \tag{13}$$

and satisfies

$$\|T_n\|_1 = 1 \tag{14}$$

$$T_n > 0 \tag{15}$$

then the thrust vector, T_w, defined by

$$T_w = T_p + (w_c v_e - \|T_p\|_1)T_n \tag{16}$$

generates the desired force F

$$F = AT_w \tag{17}$$

and the desired flow rate w_c

$$w_c = (1/v_e)\|T_w\|_1 \tag{18}$$

B. Proof

1) Show that $F = AT_w$ [Eq. (17)]. Premultiplying Eq. (16) by A yields

$$AT_w \overset{(16)}{=} AT_p + (w_c v_e - \|T_p\|_1)AT_n \tag{19}$$

$$\overset{(13)}{=} AT_p \tag{20}$$

$$\overset{(10)}{=} F \tag{21}$$

2) Show that $w_c = (1/v_e)\|T_w\|_1$ [Eq. (18)]. Taking the 1-norm of Eq. (16) yields

$$\|T_w\|_1 \overset{(16)}{=} \|T_p + (w_c v_e - \|T_p\|_1)T_n\|_1 \tag{22}$$

$$\overset{(11,15)}{=} \|T_p\|_1 + (w_c v_e - \|T_p\|_1)\|T_n\|_1 \tag{23}$$

$$\overset{(14)}{=} w_c v_e \tag{24}$$

We make the following observations regarding the Theorem in Sec. III.A.

If the net flow rate from the thrusters required to satisfy the force requirement is less than w_c [Eq. (12)], then the controller [Eq. (16)] dumps the additional flow into the null space of A.

If a thruster system works in the sense of being able to generate forces in any direction then the existence of a nonnegative null space vector, $T_n > 0$, in Eq. (15) is guaranteed by the Theorem in Sec. II.A.

Controller [Eq. (16)] is an open loop flow rate controller. This implies that the flow rate is susceptible to thruster errors. Fluctuations in flow rate result in temperature and pressure variations, however, we see in the next two sections that these temperature and pressure variations are small even if the thruster error is quite large.

As a simple example of the thruster controller [Eq. (16)], consider a configuration of three thrusters 120-deg apart in a plane. Dealing with just the forces in the plane, the configuration matrix is

$$A = \begin{bmatrix} 1 & -0.5 & -0.5 \\ 0 & 0.866 & -0.866 \end{bmatrix} \tag{25}$$

From the singular value decomposition[11] the null space is in the direction, $V_n = [0.577\ 0.577\ 0.577]'$. Normalizing by the 1-norm

$$T_n = \frac{V_n}{\|V_n\|_1} \tag{26}$$

yields a vector $T_n = [0.333\ 0.333\ 0.333]'$ which lies in the null space and satisfies Eqs. (14) and (15).

The thrust control vector, T_w, is thus given by Eq. (16), $T_w = T_p + (w_c v_e - \|T_p\|_1)T_n$, where T_p is any vector satisfying $F = AT_p$.

IV. Passive Temperature Control

The temperature of the liquid helium is self regulating. If the temperature rises then so does the pressure, forcing more flow through the thrusters and thus cooling the helium and lowering its temperature. We call this the passive temperature controller. The liquid helium temperature can also be regulated actively by measuring the temperature and controlling the net flow of helium through the thrusters to either raise or lower the temperature. We call this the active temperature controller. In this section a model of the passive temperature controller is derived and then used to predict the temperature of the liquid helium and the worst case temperature variations. In the subsequent section an active temperature controller based on this model is derived and compared to the passive system. This controller uses feedback from a thermometer immersed in the liquid helium. A potential area for future research is to compare this scheme to pressure feedback from a sensor upstream of the thrusters.

The passive temperature control model derived in this section is based on a linearization of the equations governing the states of the system. Linearization is justified in this case since the passive and active regulators always operate very close to equilibrium. Although the parameter values (Table 1) used in this section are specifically for GP-B, the model and controller are applicable in general to any system which uses the boil-off gas of a cryogenic liquid as the propellant for a thruster system. The nominal values of the states for GP-B are tabulated in Table 2.

The passive helium flow system is shown schematically in Fig. 2. Heat leaking into the dewar at a rate of $\dot{Q}_0$ causes the liquid helium to boil off at a rate of w (mg/s). The boil-off gas escapes from the dewar through a porous plug[4] and a heat exchanger to a manifold and finally out through the thrusters.

Table 1 System parameter values for GP-B

Parameter	Physical meaning	Value
h_{gl} @ 1.8 K	Vaporization heat	0.023 J/mg
k_p	Thermal resistance	1.8 K/W
k_{tp} @ 1.8 K	Pressure vs temperature	5845 Pa/K
P_{05}	Pressure drop	65.5 Pa
R_{05}	Flow impedance	241 Pa/(mg/s)
R_s	Thermal resistane	921 K/W
CM @ 95%	Thermal mass	1189×10^3 J/K
CM @ 5%		74×10^3 J/K
τ @ 95%	Time constant	2.1×10^6 s
τ @ 5%		0.13×10^6 s
R	He gas constant	2077 J/kg·K
V	Plenum volume	8.2×10^{-3} m^3
c	Plenum capacitance	0.018 mg/Pa

Table 2 Nominal values for the states

State	Physical meaning	Value
Q^n	Heat leak	0.15 W
w^n	Flow rate	6.5 mg/s
T_0^n	Liquid He temperature	1.8 K
T_s^n	Shell temp.	220 K
P_0^n	Liquid He pressure	1635 Pa
I_{sp}	Specific impulse	130 s
v_e	Exhaust velocity	1.24 km/s
η	He gas viscosity	15.8 mg/m·s
ρ	He gas density	3500 mg/m^3

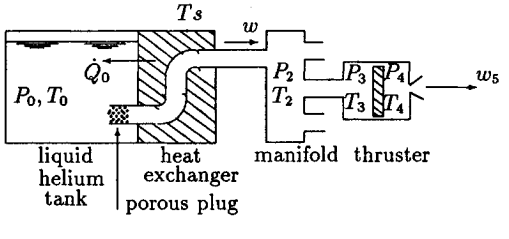

Fig. 2 Helium flow system schematic.

A. Energy Balance

The passive temperature control system is governed by the first law of thermodynamics which states that the rate at which energy is stored in a system, $\dot{E}_s$, is equal to the rate at which energy goes in, $\dot{E}_i$, minus the rate at which energy leaves the system, $\dot{E}_o$

$$\dot{E}_s = \dot{E}_i - \dot{E}_o \tag{27}$$

Energy enters the liquid helium tank in the form of heat at a rate of $\dot{E}_i = \dot{Q}_0$ watts. Energy gets taken away by the escaping helium gas at a rate of $\dot{E}_0 = h_{gl}w$ watts, where h_{gl} is the latent heat of vaporization of the helium. The stored energy inside the helium tank is proportional to the liquid helium temperature, T_0, so the rate of change of stored energy is $\dot{E}_s = CM\dot{T}_0$ where CM is the thermal mass.

Combining the expressions for $\dot{E}_0$, $\dot{E}_i$, and $\dot{E}_s$, results in the overall energy balance for the liquid helium cryogenic system

$$\dot{T}_0 CM = \dot{Q}_0 - h_{gl}w \tag{28}$$

Equation (28) also holds for small perturbations from equilibrium

$$\Delta\dot{T}_0 CM = \Delta\dot{Q}_0 - h_{gl}\Delta w \tag{29}$$

B. Pressure, Temperature, Flow Rate Relationship

The change in mass flow rate, Δw, is proportional to the change, ΔP_0, in the liquid helium supply pressure

$$\Delta P_0 = \Delta w R_{05} \tag{30}$$

where R_{05} is the overall flow impedance from inside the liquid helium tank, through the porous plug, vent lines, and out through the thrusters. The overall flow impedance, R_{05}, for GP-B is calculated in detail at the end of this section.

There is a one-to-one correspondence between the pressure, P_0, and temperature, T_0, of the multiphase vapor/liquid helium inside the tank. The variation in pressure, ΔP_0, is therefore proportional to the variation in temperature, ΔT_0

$$\Delta P_0 \approx k_{tp}\Delta T_0 \tag{31}$$

C. Temperature Variation Model

Combining Eqs. (29–31)

$$\Delta\dot{T}_0 CM = \Delta\dot{Q}_0 - \frac{h_{gl}k_{tp}}{R_{05}}\Delta T_0 \tag{32}$$

yields the fundamental relationship governing temperature variations, ΔT_0, of the liquid helium.

To understand Eq. (32), assume that there is sudden increase in heat leak, $\Delta\dot{Q}_0$, into the liquid helium tank. This results in an instantaneous temperature rise at a rate of $\Delta\dot{T}_0$ K/s. Eventually the increased temperature, ΔT_0, and corresponding increased pressure, ΔP_0, will force higher helium gas mass flow rates, Δw, through the thrusters, thus offsetting the increased heat leak by the third term in Eq. (32).

Equation (32) can be written as an input/output relationship in terms of s

$$\frac{\Delta T_0(s)}{\Delta\dot{Q}_0(s)} = \frac{k_p}{\tau s + 1} \tag{33}$$

where the thermal resistance, k_p, is

$$k_p = \frac{R_{05}}{k_{tp}h_{gl}} \tag{34}$$

Table 3 RMS Liquid helium temperature variations

Temperature control	ΔT_0, μK @ Roll frequency, 0.01 rad/s		ΔT_0, mK
	95% Full	5% Full	Steady state
Passive	1.1	17.4	22
Active	1.1	17.4	0.01

Table 4 RMS Liquid helium pressure variations

Temperature control	ΔP_0, Pa @ Roll frequency, 0.01 rad/s		ΔP_0, Pa
	95% Full	5% Full	Steady state
Passive	6.2×10^{-3}	0.1	130
Active	6.2×10^{-3}	0.1	0.06

Table 5 Disturbances

Disturbance	RMS Magnitude, 1σ	Frequency, rad/s
ΔT_s	± 5.7 K	$\leq 1.5 \times 10^{-6}$
Δw	0.27 mg/s	≥ 0.5
ΔT_m	± 10 μK	≤ 1

and the thermal time constant is

$$\tau = \frac{R_{05}CM}{k_{tp}h_{gl}} \tag{35}$$

The values k_p and τ for GP-B are listed in Table 1. The thermal resistance, k_p, gives the change in liquid helium temperature, ΔT_0, due to long term ($s = 0$) changes in heat leak, $\Delta\dot{Q}_0$. For GP-B the heat leak rate could change by $\Delta\dot{Q}_0 = 12$ mW resulting in a long term change of the liquid helium temperature of $\Delta T_0 = k_p\Delta\dot{Q}_0 = 22$ mK. This value as well as temperature variations under various other conditions are tabulated in Table 3. Pressure variations are tabulated in Table 4. The variation in heat leak, $\Delta\dot{Q}_0$, takes into account variations in the helium tank shell temperature, ΔT_s, and thruster flow rate error, Δw:

$$\Delta\dot{Q}_0 = \frac{\Delta T_s}{R_s} + h_{gl}\Delta w \tag{36}$$

The expected variations, ΔT_s and Δw, for GP-B are summarized in Table 5.

The time constant τ in Eq. (33) tells you how fast the liquid helium temperature will change. If the GP-B liquid helium tank is 95% full, for example, and the heat leak suddenly changes to a new steady-state value, then it will take roughly $\tau = 2.1 \times 10^6$ s or 24 days for the liquid helium temperature to reach $1/e$ of its equilibrium at a new steady-state value. This long time constant is consistent with the temperature variations experienced on IRAS.[12] Even though IRAS had a smaller dewar, it took over 20 days to reach the equilibrium operating temperature. The initial temperature stabilization time can be speeded up greatly with active temperature control.

Equation (33) is not just limited to predicting steady-state behavior. Since it describes the dynamics of the passive temperature control system it can be used to predict liquid helium temperature variations due to disturbances occurring at any frequency. The magnitude of Eq. (33) as a function of frequency is

$$\frac{|\Delta T_0|}{|\Delta\dot{Q}_0|} = \frac{k_p}{\sqrt{\tau^2 w^2 + 1}} \tag{37}$$

Equation (37) multiplied by $\Delta\dot{Q}_0$ from Eq. (36) and Table 5 is plotted in the convenient Bode form in Fig. 3. The magnitude of the liquid helium pressure variations can be found from Eqs. (37) and (31)

$$|\Delta P_0| = k_{tp}|\Delta T_0| \tag{38}$$

The GP-B spacecraft is particularly sensitive to temperature variations at the spacecraft roll frequency of 0.01 rad/s (one revolution every 10 min). Table 3 summarizes the worst case steady-state and roll frequency liquid helium temperature variations for GP-B. These variations were found using Eq. (37) and making the conservative assumption that all of the disturbances in Table 5 occur at either steady-state or roll frequency.

D. Steady-State Temperature Model

So far our model [Eq. (33)] only describes temperature and pressure variations from equilibrium. The complete model which also gives steady-state or equilibrium values is given by the following three equations:

$$\Delta\dot{T}_0 CM = \left(\frac{\Delta T_s}{R_s} + \dot{Q}^n + \dot{Q}_h\right) - h_{gl}w \tag{39}$$

$$wR_{05} = P_0^n + k_{tp}\Delta T_0 - P_{05} + \Delta wR_{05} + P_{\text{fep}} \tag{40}$$

$$T_0 = T_0^n + \Delta T_0 \tag{41}$$

This model gives the equilibrium values of liquid helium temperature, T_0, pressure, P_0, mass flow rate, w, as well as the variations in these quantities due to variations in shell temperature, ΔT_s, flow rate, Δw, and heater input $\dot{Q}_h$. This model is found by linearizing the thermodynamic and flow relationships about an equilibrium value. The model is accurate since the worst case variations from equilibrium are relatively small (Table 3). Table 2 lists the equilibrium values for the states.

Equations (39–41) are displayed in block diagram form in Fig. 4. An equivalent electrical circuit representation of this model is given in Fig. 5 with

$$\Delta P_0 \overset{\text{def}}{=} k_{tp}\Delta T_0 \tag{42}$$

$$P \overset{\text{def}}{=} P_0^n - P_{05} + \Delta wR_{05} + \Delta P_0 + P_{\text{fep}} \tag{43}$$

where R_{05} is the equivalent resistance of the parallel connection of thrusters in series with the porous plug and vent lines. The pressure P can be increased for emergency thrust by activating the fountain effect pump, P_{fep}.[4]

E. Pressure Drop

The helium flows through a porous plug, some heat exchangers, and vent pipes, and finally through the valves and nozzles of the thrusters as depicted in Fig. 2. The pressure

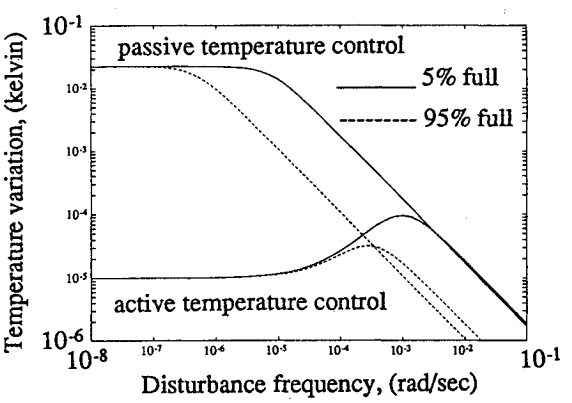

Fig. 3 Liquid helium temperature variations for the passive and active temperature controllers as a function of frequency assuming a worst case heat variation, $\Delta\dot{Q}_0 = 12$ mW.

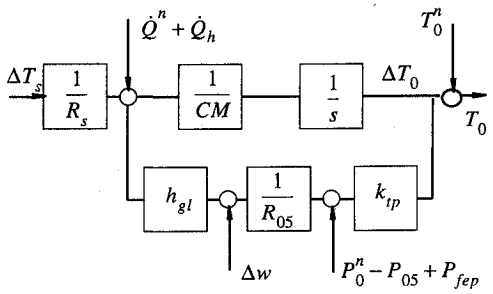

Fig. 4 Passive temperature control system block diagram.

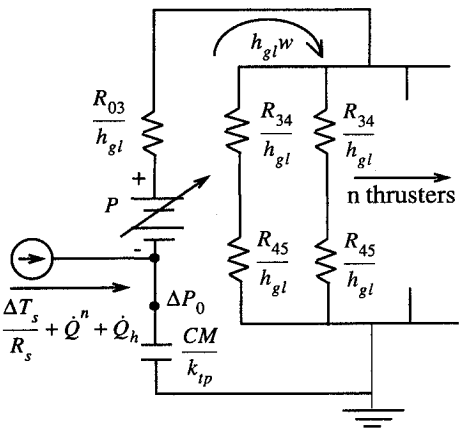

Fig. 5 Equivalent circuit depicting the thruster system thermodynamics.

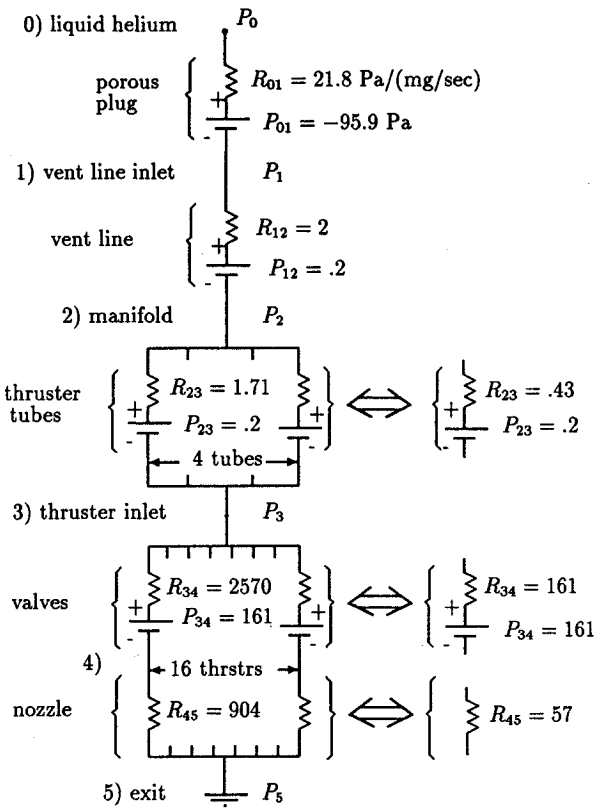

Fig. 6 Detailed pressure drop model of the helium flow system for GP-B.

drop across each stage, $P_i - P_j$, is a nonlinear function of w. We fit the linear model

$$P_i - P_j = wR_{ij} + P_{ij} \tag{44}$$

to each stage, where R_{ij} is the flow impedance between points i and j, and P_{ij} is the bias in the linear model. The overall pressure drop, $P_0 - P_5$, is the sum of the drops across each stage. This is illustrated in the equivalent circuit diagram of Fig. 6 which lists the resistances and nominal drops across each stage of the flow system. The values are calculated from a combination of experimental, analytical, and computer simulation results as follows.

1. Porous Plug

The porous plug acts as a vapor-liquid separator.[4] The temperatures of the vapor at various flow rates were measured experimentally. The output pressures are the corresponding liquid-vapor saturation pressures.[13] The coefficients R_{01} and P_{01} in Fig. 6 were found by fitting Eq. (44) to the experimental data.

2. Vent Pipes

The Reynolds numbers for the flow through the vent pipes leading from the porous plug to the thrusters are on the order of 10, therefore, the flow is highly viscous and laminar. Since the diameter of the vent pipes is large (approximately 1 cm), the Knudsen number is small and continuum flow techniques to calculate the pressure drops can be applied.[14] Assuming a constant density ρ, the pressure drop in the pipes is

$$P_1 - P_2 = R_{12}w \overset{\text{def}}{=} \left(\frac{8l\eta}{\pi r^4 \rho}\right) w \tag{45}$$

where l is the length of the line, η is the viscosity (Table 2), and r is the pipe radius. The values for R_{12}, P_{12}, R_{23}, and P_{23} in Fig. 6 come from a detailed nonlinear model of the pressure drop for GP-B,[15] however, Eq. (45) is sufficiently accurate for a preliminary assessment of the pressure drop.

3. Thrusters

The pressure drop across the valve and nozzle combination of the proportional thrusters was measured by Bull[5] and Chen.[6] The drop across the nozzle itself, P_4, is found from the isentropic relationship

$$P_4 = \frac{\sqrt{RT_s^n}}{C_d \Gamma A_t}(1 \times 10^{-6})w \overset{\text{def}}{=} R_{45}w$$
$$\Gamma = \sqrt{\gamma}\left(\frac{2}{\gamma + 1}\right)^{(\gamma+1)/2(\gamma-1)} \tag{46}$$

where $R = 2077$ J/kg·K is the gas constant for helium, $C_d = 0.7$ is the discharge coefficient,[5] $A_t = 1.47 \times 10^{-6}$ m^2 is the thruster throat area,[6] $\gamma = 1.67$ is the ratio of specific heats for helium, and w is the flow rate in mg/s. The pressure drop across the thruster valve is found by subtracting the drop across the nozzle [Eq. (46)] from the overall drop across the thruster as measured by Chen.[6] The resulting values for R_{34}, P_{34}, and R_{45} are listed in Fig. 6.

V. Active Temperature Control

The liquid helium temperature can be actively regulated by controlling the net rate of helium that flows through the thrusters. The temperature can therefore be kept constant even if the heat leak varies. The block diagram of an active temperature controller is shown in Fig. 7. A proportional-integral compensator adjusts the flow rate command w_c to make the error between the commanded temperature T_r and the measured temperature T_m as small as possible. Due to the integral term, the steady-state error is zero. The flow rate is adjusted by commanding the thrusters according to the

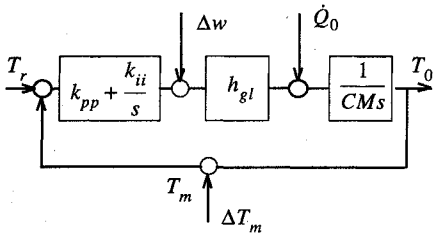

Fig. 7 Active temperature controller block diagram.

Table 6 Active temperature controller gains

	Value % Liquid volume	
Parameter	95% Full	5% Full
ω_n, rad/s	62×10^{-6}	1×10^{-3}
k_{pp}, mg/K·s	6400	6400
k_{ii}, mg/K·s^2	2×10^{-4}	3.2

thruster control law of Eq. (16) in the Theorem of Sec. III.A.

The measured temperature T_m is the sum of the true temperature T_0 plus the temperature sensor error, ΔT_m: $T_m = T_0 + \Delta T_m$. The temperature sensor is assumed to be a germanium resistance thermometer which has an accuracy published by the manufacturer of ±1 mK. The long-term stability however, once the sensor is cooled down to its operating temperature, is less than ±10 μK. This is the value tabulated in Table 5 for temperature sensor error, ΔT_m.

The block diagram of Fig. 7 is represented by the following two transfer functions:

$$\frac{T_0(s)}{T_r(s) + \Delta T_m(s)} = \frac{k_a(k_{pp}s + k_{ii})}{s^2 + k_a(k_{pp}s + k_{ii})} \tag{47}$$

$$\frac{T_0(s)}{\Delta\dot{Q}(s)} = \frac{s/CM}{s^2 + k_a(k_{pp}s + k_{ii})} \tag{48}$$

where

$$k_a = \frac{h_{gl}}{CM}$$

The transfer function $T_0/\Delta\dot{Q}$ has a maximum of

$$\left(\frac{T_0}{\Delta\dot{Q}}\right)_{\max} = \frac{1}{2CM\omega_n} \tag{49}$$

at the control bandwidth of

$$\omega_n = \sqrt{k_a k_{ii}} \tag{50}$$

Equation (49) can be used to choose the control gains, k_{ii} and k_{pp}, which are summarized in Table 6. First, ω_n is picked to guarantee that the temperature does not vary by more than some specified amount (e.g., ±1 mK) assuming that all of the disturbance (Table 5) occurs at the control bandwidth, ω_n. The integral gain, k_{ii}, is then found from Eq. (50) and the proportional gain, k_{pp}, is picked to give critical damping, $\omega_n = k_a k_{pp}$.

The low bandwidth of the temperature control system (Table 6) keeps it from interfering with the attitude and translation control systems, it also attenuates the response of the temperature control system to temperature sensor noise.

VI. Comparison of Active vs Passive Temperature Control

A comparison of the worst case liquid helium temperature variations for the passive and active temperature controllers is plotted in Fig. 3. This plot is conservative in the sense that it gives the temperature variations which would result at any frequency if a worst case disturbance of $\Delta\dot{Q}_0$ occurred at that frequency. The worst case disturbance, $\Delta\dot{Q}_0$, is due to the sum of the disturbances in Table 5 using Eq. (36). The curve in Fig. 3 for the passive temperature controller is found by inputting $\Delta\dot{Q}_0$, into the transfer function [Eq. (33)]. The active temperature controller curve comes from the sum of Eqs. (47) and (48). Notice that the worst case liquid helium temperature variations at low frequencies exactly track the temperature sensor variation, ΔT_m, in Table 5.

Due to the low bandwidth of the active temperature controller, the temperature variations of the passive and active controllers at the GP-B roll frequency of 0.01 rad/s are identical. In other words, the active temperature controller is operating open loop at this frequency.

The RMS liquid helium temperature and pressure variations of the passive and active temperature control systems for GP-B are summarized in Tables 3 and 4. The steady-state variations of the active system are entirely due to the temperature sensor error. We see from the tables that the passive system does an excellent job of regulating the temperature even under the worst case conditions. There are some advantages, however, to active control as summarized below.

A. Performance

The active system greatly reduces long term seasonal temperature variations. At the GP-B roll frequency of 0.01 rad/s, however, the active and passive systems both have the same temperature variation. In other words, the active temperature controller does not introduce any temperature fluctuations from sensor noise at this critical frequency. The worst case liquid helium temperature variation at roll frequency is 17.4 μK rms even with the tank only 5% full of liquid helium. This should not cause any interference to the GP-B science gyro readout electronics. Since the peak force output of the thrusters is proportional to the supply pressure it is important that the pressure remain relatively constant. The nominal pressure at 1.8 K is 1635 Pa. From Table 4, the worst case pressure variation of the passive system, 130 Pa, corresponds to an 8% variation in the peak force output of the thrusters. For the active system the corresponding worst case thrust variation is only 0.4%. The point is that the active temperature controller maintains a constant liquid helium temperature and pressure even with varying heat loads.

B. Simplicity

The "actuator" for the active system is automatically in place: it is simply the net flow rate command to the thruster controller in Eq. (16) of the Theorem in Sec. III.A. The sensor for the active system is also available since a liquid helium temperature sensor is required even if active temperature control is not implemented. The only complexity added by active temperature control is the controller itself which in this case is a simple proportional-integral compensator with a time constant greater than 1 h. A digital implementation of this controller needs to be updated only several times an hour.

C. Uncertainties

There are uncertainties in the expected shell temperature, heat leak rate, flow resistance, initial transients, and the atmospheric drag. The actual temperature at which the passive system will reach equilibrium is hard to predict. As with any feedback system the active temperature controller is much less sensitive than the passive system to the uncertainties, and it is therefore much easier to predict accurately the steady-state condition of the active system.

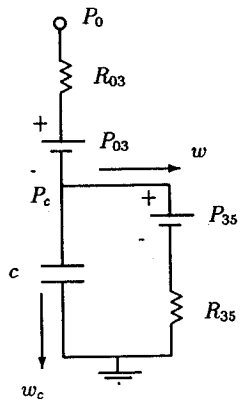

Fig. 8 Equivalent circuit of plenum pressure, P_c, dynamics.

D. Dynamic Range

The dynamic range of the thrusters can be adjusted by changing their supply pressure. Once the spacecraft is in orbit the active temperature controller can adjust the temperature so that the corresponding pressure will result in peak thruster outputs which are tuned to the true disturbance environment.

VII. Plenum Pressure

The volume of the vent lines and manifolds downstream of the porous plug, guard tank, and heat exchangers for GP-B is approximately $V = 8.2$ l. Assuming the average density ρ, given in Table 2, this corresponds to 28 mg of helium gas. If the nominal flow rate, w^n, listed in Table 2 increases by 10% (0.65 mg/s) what will happen to the plenum pressure upstream of the thrusters? The answer can be found by studying the equivalent circuit of Fig. 8.

The pressure drop, P_{03}, and impedance, R_{03}, are the sum of the drops across the porous plug and vent lines (Fig. 6). Similarly, P_{35} and R_{35} correspond to the overall pressure drop across the thrusters. The capacitance c is derived from the perfect gas law

$$\rho = (P_c/RT_s^n) \tag{51}$$

Differentiating both sides yields

$$\dot{\rho} = (\dot{P}_c/RT_s^n) \tag{52}$$

where $\dot{\rho}$ is the rate of change of density inside the plenum and is equal to

$$\dot{\rho} = (w_c/V) \tag{53}$$

where w_c (mg/s) is the rate at which mass is stored in the plenum. Substituting Eq. (53) into Eq. (52) yields

$$w_c = (V/RT_s^n)(1 \times 10^6)\dot{P}_c \overset{\text{def}}{=} c\dot{P}_c \tag{54}$$

The value for c for GP-B is listed in Table 1.

The plenum pressure, P_c, from Fig. 8 is given by

$$P_c = \frac{1}{\tau_c S + 1}(P_0 - P_{03} - R_{03}w) \tag{55}$$

where $\tau_c = R_{03}c$ is the time constant and has a value of less than half a second for GP-B. Since the time constant of the passive liquid helium temperature loop is at least five orders of magnitude slower than this, we can consider P_0 as a constant for the dynamics of the pressure loop. What happens to the plenum pressure if the output flow, w, suddenly increases? In about 1 s the plenum pressure reaches the new equilibrium value

$$P_c = P_0 - P_{03} - R_{03}w \tag{56}$$

For GP-B, if the flow rate increases by 10% then the plenum pressure drops by only 1%.

VIII. Conclusion

An overall thermodynamic model of a liquid helium propulsion system is derived. With a fixed output flow impedance, it is shown that the system is a natural, passive temperature regulator. The liquid helium temperature can also be actively regulated by varying the flow impedance, and therefore, the net mass flow rate through a set of thrusters. The thermodynamic model and controller are applied to the propulsion system for the GP-B spacecraft. For GP-B we can expect long term liquid helium temperature variations of 22 mK rms for the passive temperature control system. This is greater than the current requirement of ± 10 mK. The temperature variation for the active temperature controller is governed by the stability of the temperature sensor. A stability of ± 10 μK is reasonable for a germanium resistance thermometer, so the liquid helium temperature can be regulated by three orders of magnitude better than the passive system. The long term liquid helium pressure variations for the passive system are ± 130 Pa. This corresponds to roughly an 8% variation in supply pressure for the thrusters. This is unacceptably high since the thrusters for GP-B need to be calibrated to better than 1% accuracy. The long term pressure variations for the active temperature controller are again more than three orders of magnitude smaller. The GP-B experiment is very sensitive to temperature variations at the spacecraft roll frequency of one revolution every 10 min (0.01 rad/s). Due to the very long thermal time constant of the system, the worst case liquid helium temperature variation at the GP-B roll frequency is 17.4 μK rms even with the tank only 5% full of liquid helium. This should not cause any interference to the GP-B readout electronics.

References

[1]Turneaure, J. P., Everitt, C. W. F., and Parkinson, B. W., "The Gravity Probe B Relativity Gyroscope Experiment: Approach to a Flight Mission," *Proceedings of the Fourth Marcel Grossman Meeting on General Relativity*, edited by P. Ruffini, Elsevier, 1986.

[2]Worden, P. W., "Satellite Test of the Equivalence Principle," *Proceedings of the First William Fairbank Conference on Relativistic Gravitational Experiments in Space*, Rome, Italy, Sept. 1990.

[3]Fairbank, J. D., Deaver, B. S., Everitt, C. W. F., Michelson, P. F., and DeBra, D. B., *Near Zero, New Frontiers of Physics.*, W. H. Freeman and Company, New York, 1988.

[4]Everitt, C. W. F., "Report on a Program to Develop a Gyro Test of General Relativity in a Satellite and Associated Control Technology," Stanford Univ. Rept., Stanford, CA, June 1980.

[5]Bull, J. S., Precise Attitude Control of the Stanford Relativity Satellite, Ph.D. Dissertation, Stanford Univ., SUDAAR 452, Stanford, CA, 1973.

[6]Chen, J-H., Helium Thrustor Propulsion System for Precise Attitude Control and Drag Compensation of the Gravity Probe B Satellite, Ph.D. Dissertation, Stanford Univ., SUDAAR 538, Stanford, CA, 1983.

[7]Lee, K-N., The Design of a Wide Dynamic Range Helium Thruster for Gravity Probe B, Ph.D. Dissertation, Stanford Univ., Stanford, CA, 1992.

[8]Wiktor, P. J., and DeBra, D. B., "The Minimum Control Authority of a System of Actuators with Applications to Gravity Probe B," 14th Annual AAS Guidance and Control Conf., American Astronautical Society, Keystone, CO, Feb. 1991.

[9]Wiktor, P. J., The Design of a Propulsion System Using Vent Gas from a Liquid Helium Cryogenic System, Ph.D. Dissertation, Stan-

ford Univ., Stanford, CA, June 1992.

[10]Salisbury, J. K., Kinematics and Force Analysis of Articulated Hands, Ph.D. Dissertation, Stanford Univ., Stanford, CA, 1982.

[11]Strang, G., *Linear Algebra and its Applications*, Harcourt Brace Jovanovich, Inc., San Diego, CA, 1988.

[12]Urbach, A. R., Hopkins, R. A., and Mason, P. V., "One Year of Stars, Provided by the IRAS Cryogenic System," ESA/CNES Symposium on Environmental and Thermal Control for Space Vehicles, Toulouse, France, Oct. 1983.

[13]McCarty, R. D., "The Thermodynamics Properties of Helium II from 0 k to the Lambda Transition," *National Bureau of Standards Technical Note 1029*, Dec. 1980.

[14]Moody, L. F., "Friction Factors for Pipe Flow," *Transactions of the American Society for Mechanical Engineers*, Vol. 66, 1944, p. 671.

[15]Liu, C. K., "Gaseous Helium Pressure at Inlet of GP-B Thrusters, GP-B 4," Lockheed Missiles and Space Company Interdepartment Communication, Palo Alto, CA, Aug. 1989.

[16]Blount, D. H., "Attitude Control and Drag Compensation Propulsion System for the Gravity Probe B Spacecraft," NASA TM-82517, 1983.